TEMPORAL LAG EFFECTS OF ALLUVIAL SYSTEM UNDER UNSTEADY FLOW CONDITIONS

Arie Setiadi Moerwanto

Pusat Penelitian dan Pengembangan Sumber Daya Air
Jl. Ir. H. Juanda no. 193, Bandung
E-Mail: ariemoerwanto@yahoo.com

Diterima: 10 Maret 2011; Disetujui: 11 Mei 2011

ABSTRAK

Analisis perubahan morfologi sungai pada kondisi aliran tidak langgeng menuntut suatu submodel numerik yang dapat secara cermat menyimulasikan kelambanan respons temporal sistem aluvial. Pada kondisi hidrodinamika yang berubah sangat cepat, corak dasar sungai tidak dapat secara serentak merespons perubahan tersebut. Karena corak dasar sungai sangat terkait erat dengan laju angkutan sedimen dasar, maka keberhasilan pemodelan kelambanan temporal sistem aluvial akan meningkatkan ketelitian analisis perkembangan corak dasar sungai, prediksi tinggi muka air, laju angkutan sedimen dasar maupun layang dan pada akhirnya akan meningkatkan ketelitian analisis perubahan morfologi sungai. Tulisan ini membahas secara rinci cara pemodelan numerik efek-efek kelambanan temporal sistem aluvial menggunakan metode elemen hingga termasuk pengujian unjuk kerja model.

Kata Kunci: *Kelambanan respon temporal, sistem aluvial, metoda elemen hingga, aliran tidak langgeng, corak dasar sungai.*

ABSTRACT

Analysis of response of river morphology under unsteady conditions requires the strong support of the sub-model that able to simulate the temporal lag effects of alluvial system. Under unsteady flow conditions, the bed forms of an alluvial stream do not immediately respond to the change in flow conditions. Since the configuration and geometry of bed forms are integrally linked to the bed load sediment transport, in turn the accuracy of simulating the alluvial temporal lag effects will also influence the accuracy of analysis of flow depth, the bed load transport rate, the suspended load concentration and later on river morphology changes. This paper describes in detail the modelling method of temporal effects of alluvial system, to include testing of model performance in simulating those phenomena.

Keyword: *Temporal lag response, alluvial system, finite element method, unsteady flow conditions, bed forms.*

INTRODUCTION

Under unsteady flow conditions, the bed forms of an alluvial stream do not immediately respond to the change in flow conditions. This time delay in morphological adjustment is the temporal lag of the alluvial stream. The bed forms need an adaptation time to change their geometrical properties. Since the configuration and geometry of bed forms are integrally linked to the bed load sediment transport, the alluvial temporal lag effects also influence the flow depth, the bed load transport rate and the suspended load concentration. Whereas a spatial lag in the bed load transport can occur even under steady flow conditions (Moerwanto, 2010), the temporal lag effects of bed load can only occur under unsteady flow conditions

Figure 1 illustrates the schematisation of the idealised relation between the impulse discharge hydrograph, the water depth, the bed load transport rate and the equivalent steady discharge. When the flow changes rapidly, the water depth, geometric dimensions of the bed forms and the bed load transport rate cannot be directly linked to the instantaneous hydraulic conditions. Consequently, a bridging equivalent discharge is required in which its hydraulic conditions determined under steady conditions can be used to predict the actual

values of the bed roughness and bed load transport capacity which occur under unsteady flow conditions.

Adopting the temporal lag phenomenon of alluvial system allows the developed model for analysing the river morphology respond to be run under unsteady flow conditions.

AIMS

This study is aimed to develop a sub-numerical model that able to simulate the temporal lag effects of alluvial system under unsteady flow conditions using finite element method. Furthermore, the study is being carried under a scheme of the development of A Riverine Fully Coupled Finite Element Model with Sediment Transport Sub-processes as a required tool to support the adaptation policy to respond to the global climate change. To achieve those aims, the model has been setup by considering the following aspects:

1) the adoption of the dynamic wave approach by retaining all the terms in the momentum equation,
2) the explicit separation of the bed load and the suspended load transport,
3) the vertical exchange of sediment and armored layer development and a means of handling non-uniform distribution of bed material, and
4) incorporating the spatial and temporal lag effects of bed load transport as a consequence of adoption of the dynamic wave approach.

LITERATURE REVIEW

Based on the data from a series of steady and unsteady flume experiments, a general temporal lag model to predict values of the bed roughness and sediment transport capacity under unsteady flow conditions has been proposed by Phillips et al. (Phillips, 1984; Phillips and Sutherland, 1989). The basis of this model is the equivalence between the morphological conditions (e.g. bed roughness and bed load transport rate) developed under unsteady flows and the steady discharge that can be used to reproduce the same morphological conditions. The values of the bed roughness and sediment transport capacity under unsteady flows are predicted by the method given in Figure 2.

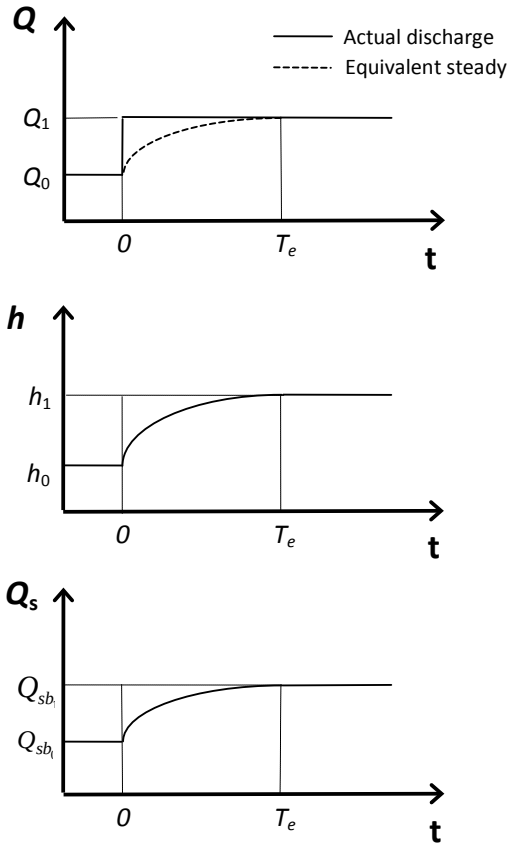

Figure 1 Schematisation of the temporal lag effect of the alluvial stream (adapted from Phillips, 1984).

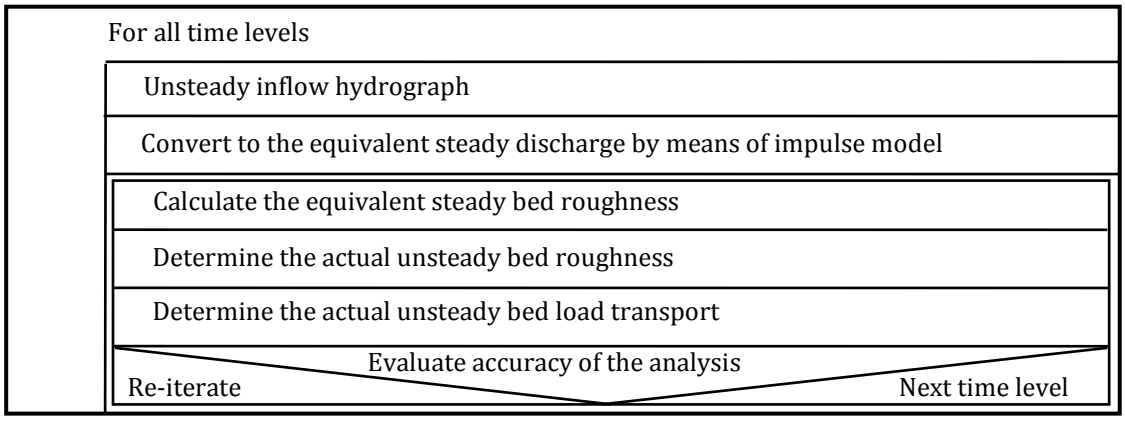

Figure 2 Structure diagram of the temporal lag model.

The unsteady flow hydrograph is converted into a series of equivalent steady discharges which are used to size the bed forms and to estimate the bed load transport rate. The equivalent steady discharge is determined as follows (Phillips, 1984; Phillips and Sutherland, 1989):

$$Q_e = Q_{base} + \sum_{i=1}^{n} a_{Q_i} \left[\left(t - t_{0_i} \right) + T_{e_i} \ln \left(\frac{T_{e_i}}{T_{e_i} + t - t_{0_i}} \right) \right] \qquad \textbf{(1)}$$

$$T_{e_i} = \frac{0.0295}{\sqrt{\Delta g D_{50}{}^3 \theta_c}} \frac{h_e{}^2}{\theta} \qquad \textbf{(2)}$$

where

a_{Q_i} , slope of the i[th] discharge limb in the superposition solution as illustrated in Figure 3, [m^3/s^2];

D_{50} , bed material particle diameter for which 50 % is finer, [m];

he , equilibrium flow depth after unsteady effects have dissipated, [m];

n , r for $t_{0_r} < t < t_{0_{r+1}}$;

Q_e , equivalent steady discharge at time t , [m3/s];

Q_{base} , initial discharge, [m^3/s];

T_{e_i} , a modified equivalent steady discharge time scale of i[th] discharge limb, [s];

t_{0_i} , time at which the i[th] discharge limb commences, [s];

Δ , relative density for submerged bed material, [-].

The bed load transport rate and bed roughness are integrally linked because bed forms are a part of the bed load transport mechanism. The linkage which exists between the bed load transport rate and bed roughness under steady flow conditions is also assumed by Phillips (1984) and Phillips and Sutherland (1989) to exist under unsteady flow conditions. Hence, it is assumed that the same bed roughness in unsteady flows can also be derived by the equivalent steady flow. The existing bed roughness predictors can then be used in combination with the equivalent steady flow discharge. Similarly, the existing formulas for estimating bed load transport capacity can be used in combination with the equivalent steady flow to estimate the bed load transport in unsteady flows.

The friction factor is composed of the grain-related part f', and the bed form-related part f''. This composition influences the response of the bed roughness due to unsteady flows. Based on his experiments, Goodwin (1986) distinguished the following two stages of the alluvial response, (i.e. primary and secondary), due to a sudden change in discharge as (see Figure 4):

The sudden changes in water depth from h_0 to h_1, and in bed load sediment transport rate from Q_{sb_0} to Q_{sb_1}, are caused by the inability of alluvial system to respond instantaneously to the change in flow conditions. Hence initially, the effective alluvial bed roughness at the new flow Q_2, is a combination of the grain related part at the new discharge and the bed forms developed under the former discharge Q_0. These changes are termed the primary changes.

As the new bed forms gradually develop, the effective bed roughness becomes larger and in turn the water depth and bed load transport rate also adjust to their new equilibrium values h_2 and Q_{sb_2}. These gradual changes are termed as the secondary changes.

Temporal lag effects will also occur when there is a sudden decrease in the discharge. In the case of wide channels, the water depth in the primary phase h_1, can be obtained, for example, by the following approach due to Einstein based on the Darcy-Weisbach equation:

$$(h_1)^3 = \mathrm{f}_1 \frac{(q_2)^2}{8\, g\, I_0} = \left(\mathrm{f}_1^{'} + \mathrm{f}_0^{''}\right)\frac{(q_2)^2}{8\, g\, I_0} \qquad \textbf{(3)}$$

The grain-related part of the friction factor, $\mathrm{f}_1^{'}$, can be estimated from the following relation due to Einstein:

$$\mathrm{f}_1^{'} = 8\left(\frac{u_*^{'}}{u}\right)^2 = 2.5\ln\left(\frac{h_1}{D_{65}}\right) + 6.0 \qquad \textbf{(4)}$$

The bed form-related part of the friction factor $\mathrm{f}_0^{''}$, for the former flow q_0, can be estimated, for example, by using the form friction factor of Darcy-Weisbach for dunes as proposed by Engelund (van Rijn, 1993):

$$\mathrm{f}^{''} = 10\frac{H^2}{h\,\lambda}\left(e^{-\left(\frac{2.5H}{h}\right)}\right) \qquad \textbf{(5)}$$

Substituting $\mathrm{f}_1^{'}$ and $\mathrm{f}_0^{''}$ into Equation (3) yields a result for h_1 which lies in the range between the water depth associated with the former discharge h_0, and the water depth corresponding to the new discharge h_2.

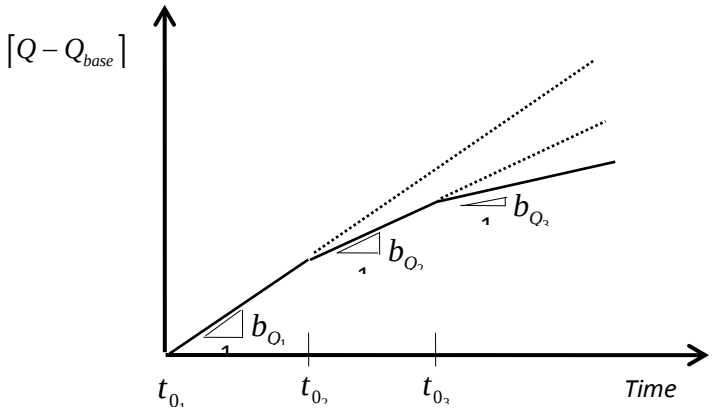

a) Discharge hydrograph

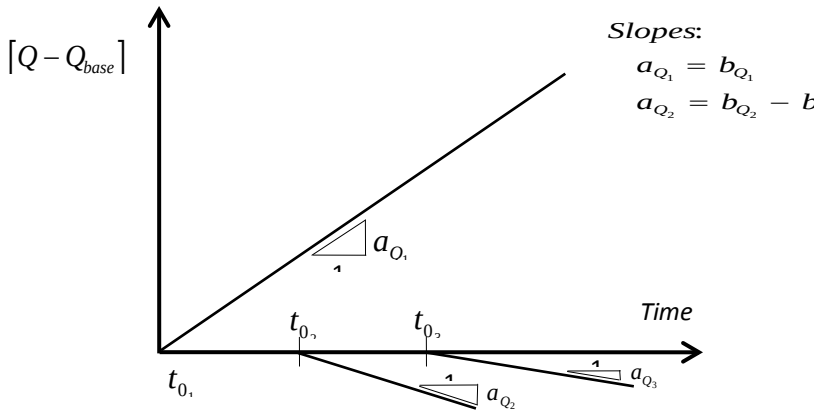

b) Superposition of the flows

Figure 3 Superposition solution for a complex inflow hydrograph (after Phillips, 1984).

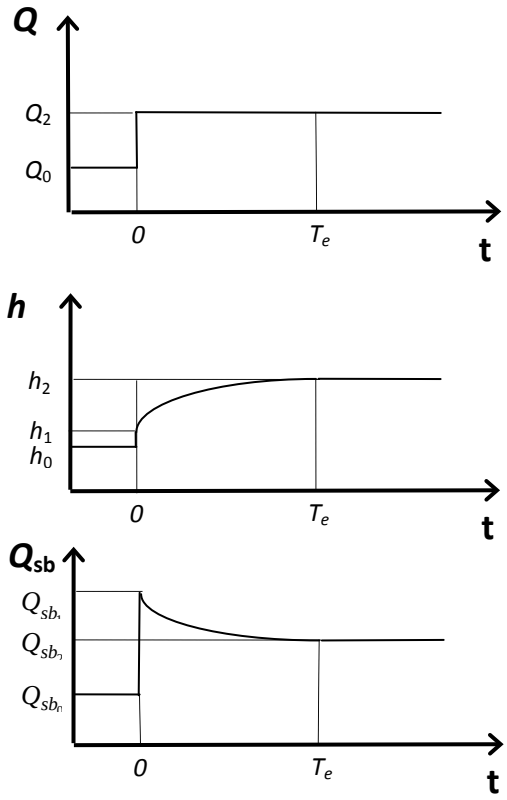

Figure 4 Schematisation of the temporal lag effect of the alluvial stream (adapted from Goodwin, 1986).

Furthermore, t_{90} which is defined as the time required for ninety percent of the change between h_1 and h_2 to be completed, is introduced to describe the temporal variation of water depth changes. Considering the equilibrium sizes of the bed forms and the equilibrium bed load transport rate at the former and new discharge conditions, (i.e. q_0 and q_2), the following empirical relation was proposed to determine t_{90} (Goodwin, 1986):

$$t_{90} = 0.36\,(1-p)\rho_s \frac{\Delta H \,.\, \frac{1}{2}\left(\lambda_1 + \lambda_2\right)\, \overline{c}_2^{\,0.75}}{q_2 \qquad \Delta\, \overline{c}^{\,1.75}} \quad \textbf{(6)}$$

where

$\overline{c}_2$, bed load sediment concentration at the new equilibrium conditions, [kg/m^3];

$\Delta\overline{c} = \overline{c}_2 - \overline{c}_0$, the difference between the bed load sediment concentration of the two discharge conditions, [kg/m^3];

$\Delta H = H_2 - H_0$, the difference between the bed form heights of the two discharge conditions, [m];

q_2, the new water discharge proceeding to the alluvial reach, [m^3/s/m];

λ, wave length of the bed forms, [m].

By using t_{90} the time variation of the water depth and the bed load transport rate can be evaluated. At this stage, the derivation of the temporal lag effects on h and Q_{sb} for an alluvial stream appears to have the correct form. From Equation (6), it can be seen that if $\Delta\overline{c}$ is small, then t_{90} becomes large. Further, if ΔH is large, a larger volume of bed material must be transported and t_{90} increases. However, with probing it can be seen that Goodwin's work contains a contradiction which is examined below:

Using the temporal variation of the water depth and the imposed discharge change data, the bed load transport rate can be computed by, for example, the following relation:

$$q_{sb}(t) = a\left(\frac{q_2}{h(t)} - u_{cr}\right)^b, \quad \textbf{(7)}$$

where coefficient a and exponent b are constant, u_{cr} is the critical velocity for the initiation of motion. This computation results in the temporal variation of the bed load transport rate as schematised in Figure 4.

Referring to Figure 4, the sudden jump in bed load transport rate should be followed by an immediate change in bed forms. However, the sudden jump in water depth, i.e. from h_0 to h_1 in Figure 4 represents the lag of bed form development due to a temporal lag of the bed load transport. Therefore, the time variation of the bed load transport rate and the development of bed forms are not in a reasonable agreement.

Due to the embedded contradiction in Goodwin's model for the temporal lag of an alluvial stream, only the equivalent steady discharge approach proposed by Phillips will be further elaborated in the present study.

METHODOLOGY

This present study is carried out to support the development of A Riverine Fully Coupled Finite Element Model with sediment transport sub-processes. To achieve an efficient and robust sub-model that could easily communicate with the main model, the structure of sub-model for analyzing temporal lag effects of alluvial system is also designed by implementing the modularity advantages of finite element solution. The performances of the sub-model are steps by steps verified by comparing its prediction results with set of data resulted from physical hydraulic laboratory tests.

Setting Up of Temporal lag effects of Alluvial System as a Part of Bed Load Sediment Transport Sub-Model. To achieve the desirable model, the following two field phenomena of bed load transport are incorporated and simulated by the bed load transport sub-model: The bed load sediment transport capacity under unsteady flows is analyzed by including the temporal lag effects of the alluvial reach. For this purpose, simulation is carried out by adopting Equations (1) and (2),

The actual bed load sediment transport rate is analyzed by including the spatial lag effects of the bed load transport (Moerwanto, 2010). The structure diagram of the designed bed load transport sub-model as a subroutine of the being developed A Riverine Fully Coupled Finite Element Model with Sediment Transport Sub-processes is presented in Figure 5.

ASSESSMENT OF COUPLED MODEL FOR SIMULATING THE TEMPORAL LAG EFFECTS OF ALLUVIAL STREAMS

The series of tests carried out have the objective of determining any advantage of incorporating the temporal lag effects of alluvial streams into the present model. For this purpose, three series of the flume experiments conducted by Bell (Bell, 1980; Bell and Sutherland, 1983) are simulated by the present model. The non-equilibrium sediment transport conditions were created by enforcing zero sediment input at the upstream boundary of the test reach. The unsteady flow conditions were created by super imposing a symmetrical flood wave on a steady base discharge. Consequently, both the spatial and temporal lag effects were present.

To determine the effects of incorporating the temporal lag sub-model in the present model, the numerical model with the coupled solution method is applied to simulate Bell's experiments. The first series of simulations are carried out by using the model that incorporates the spatial lag module only. Later, the second series of simulations are conducted by the model that incorporates both the spatial and temporal lag modules.

1 Model simulations

1) Schematisation of the flume experiments

The simulations are carried out with the same nodal layout as shown in Figure 6. Twenty four non-uniform elements are used to represent the flume. The space steps range from 0.25 m for the upstream elements to 20 m for the downstream elements.

Reorganize all data transferred from the primary model
For all sediment size classes
For all the elements
Evaluate the exposure correction factor
Calculate the total load sediment transport capacity
Calculate the ratio of the bed load to the total load sediment
Evaluate the actual bed load sediment transport rate by taking into account the spatial and temporal lag effects of alluvial system
Return to the primary model

Figure 5 Structure diagram of the bed load sediment transport sub-model.

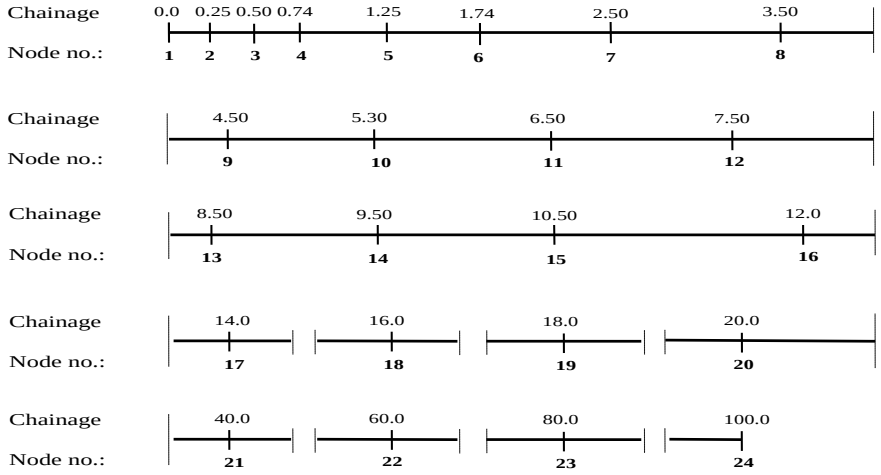

Figure 6 Chainage along flume and element configuration of the numerical model.

2) Initial conditions

a) The bed is initially plane with a constant bed slope of I_0 = 0.002. This slope is also used as the initial friction slope since the flow is initially uniform.

b) The initial flow conditions are a constant base discharge and uniform flow depth of h = 0.077 m over the entire length of the flume. The base discharge is determined based on the critical conditions for the initiation of particle sediment motion. Considering the initial bed slope, the side walls correction and bed material data, the initial base discharge of q = 0.0374 $m^3/s/m$ is used (Bell, 1980).

c) The bed load transport is initially zero over the entire length of the test reach since the base water discharge is just at the threshold of motion as discussed above.

3) Upstream boundary conditions

a) The hydrodynamic boundary condition at the upstream end consisted of one of three types of flood wave hydrograph superimposed on the base discharge. The hydrographs are displayed in Figure 7. The maximum discharge per unit width of the flume for each flow hydrograph is:

- NS02 experiment: $q_{max}(x=0,\ t=600)$ = 0.160 $m^3/s/m$,
- NS03 experiment: $q_{max}(x=0,\ t=1200)$ = 0.097 $m^3/s/m$,
- NS06 experiment: $q_{max}(x=0,\ t=2400)$ = 0.160 $m^3/s/m$.

b) The imposed, upstream bed load transport boundary condition is

$$q_{sb}(x=0,\ t\geq 0) = 0.0\ m^3/s/m$$

Bell (1980) noted that no sediment particles were transported as suspended load. Therefore, the advection-diffusion equation for suspended load can be omitted and no boundary conditions related to this equation are required.

4) Downstream boundary conditions

A downstream hydrodynamic boundary condition is required for subcritical flows. This entails specifying a primary variable or a *Q-h* rating curve at the downstream end. In these model simulations, a *Q-h* curve is specified at the downstream boundary.

2 Test results and discussion

The results of the model with the coupled solution method for the NS02, NS03 and NS06 laboratory experiments of Bell are displayed in Figures 8 to 10. These figures also contain the measured time variation of the bed load transport rate at flume chainages x = 0.74, 1.74, 3.5, 5.3 and 9.3 *m*. The spatial lag effects are included in the results of all the models runs and presented in Figures 8 to 10.

The effect of incorporating the temporal lag effect module is evident. For the NS02 test with its steep hydrograph at the upstream boundary, the temporal lag module reduces the peak of the predicted bed load transport rate to almost a half compared with the module prediction which only incorporates the spatial lag effect module. Apart from the results at chainage x = 0.74 *m*, the prediction with both temporal and spatial lags yields the best match with the measured data. The reduction in the peak bed load transport rate is smaller for the cases with a gentler inflow hydrograph. The test results also show that incorporating the temporal lag module causes a delay in the peak of the bed load transport rate. For test series NS02 this delay is as long as about 100 seconds, i.e. 8.3% of the duration of the imposed flood wave. This phenomenon is also evident in the measured data.

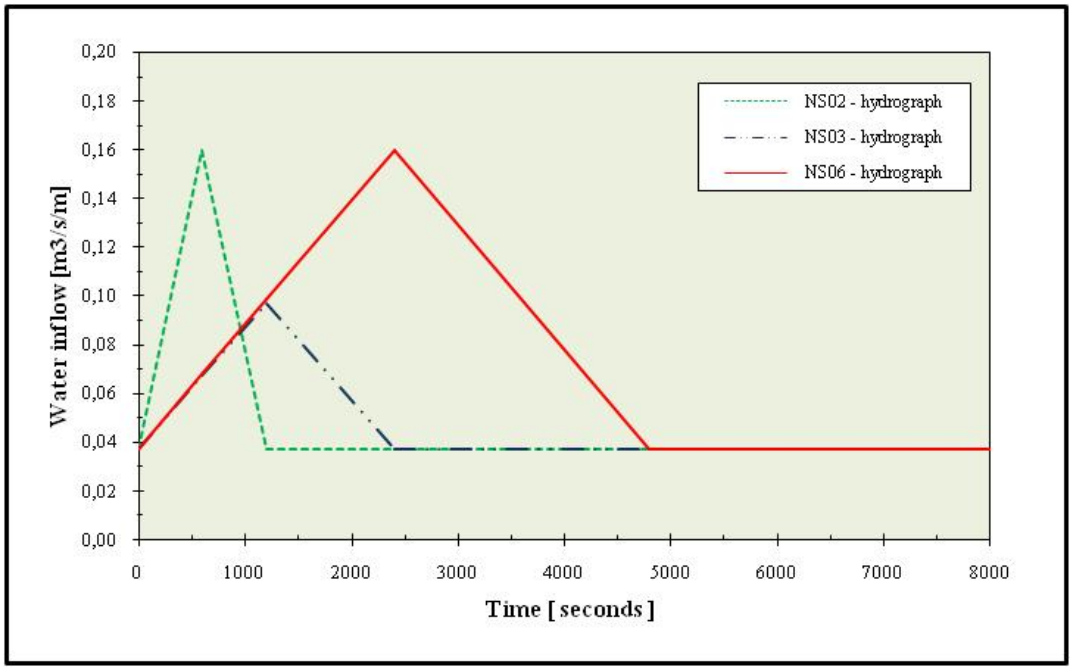

Figure 7 Three inflow hydrographs used by Bell (1980) in the flume experiments

Table 1 contains the total weight of the eroded sediment predicted at flume chainages x = 0.74, 1.74, 3.5, 5.3 and 9.3 *m*. The flume data measured during the flood passage is also included in the table as a comparison. It is evident from this table that in general, the predicted results given by the module with both temporal and spatial lag modules agree reasonably well with the measured data, i.e. generally within about 35%.

The present model tends to underestimate the bed load transport rate at the chainage x = 0.74 *m*. This tendency is particularly evident in the NS02 and NS03 series of tests. This lack of agreement may be caused by the following reasons:

a) A fluid vortex just downstream of the fixed bed causes a local scour hole at the interface between the fixed and moveable beds. The scoured bed material from this region contributes an additional amount to the transported sediment. This additional transport cannot be predicted by the bed load transport sub-model. An attempt has been made to account for this scour mechanism. A module to predict the scour depth and volume of the scoured material due to the vortex has been incorporated as discussed by Moerwanto (2010). However, it is evident in these series of tests that the effectiveness of this module to predict the volume of scoured material is not satisfactory.
b) The difficulty in measuring the bed load transport rate at chainage x = 0.74 *m* is a problem that may influence the quality of the measured data. This chainage is located in a section where the bed level changes rapidly. Therefore, it is difficult to correctly placed the mouth of the bed load collectors.

   This possibly poor data could be improved by carrying out many additional tests and follow up by the usage of statistical analysis.

   Considering the rate of increment of hydrograph used in NS02 series of test is sharper to compare with NS06 series. Taking into account this input in evaluating the performances of the model to predict the sediment transport rate under those conditions, one may conclude that there is still room for improvement in adopting the equivalent steady discharge approach for modeling the temporal lag effect. However, for the purpose of simulating field conditions, where a such sharp discharge hydrograph is rarely found, it could be alleged that the model performance is satisfied.
c) The temporal lag effect of the bed load transport module has reduced the celerity of bed disturbances during flashy flows and hence also the magnitude of dimensionless transport parameter, Ψ. As a result, the difference between the celerity of a disturbance on the water-sediment interface on the channel bed compared to that on the air-water interface becomes higher. This bed load characteristic tends to widen the range of applicability of the model with a decoupled solution method.
d) Since the bed material transport and geometry of bed forms are integrally linked to each other,

hence the accuracy of simulating those phenomena under unsteady conditions will also influence the accuracy of analysis of flow depth in rivers, the passage of flood hydrographs and later on the river morphology changes. Hence, this study results is supposed to contribute in perfecting the numerical modeling of hydrodynamics as well as analysis of river morphology response.

Table 1 Summary of measured and predicted total eroded sediment during each flood passage

Series	Chainage [m]	Total transported sediment [kg]		
		Spatial Lag	Spatial + Temporal	Measured
NS02	0.74	4.797	2.243	4.57
NS02	1.74	5.440	2.376	2.28
NS02	3.50	5.557	2.384	2.61
NS02	5.30	5.563	2.381	3.28
NS02	9.30	5.564	2.374	3.86
NS03	0.74	2.710	1.845	2.62
NS03	1.74	2.793	1.875	1.40
NS03	3.50	2.797	1.875	1.70
NS03	5.30	2.797	1.875	2.36
NS03	9.30	2.797	1.875	2.24
NS06	0.74	19.188	14.918	7.91
NS06	1.74	21.762	16.490	12.20
NS06	3.50	22.228	16.707	17.15
NS06	5.30	22.254	16.716	16.70
NS06	9.30	22.253	16.716	17.90

Note: S = incorporating spatial lag module only
S + T = incorporating spatial and temporal lag modules

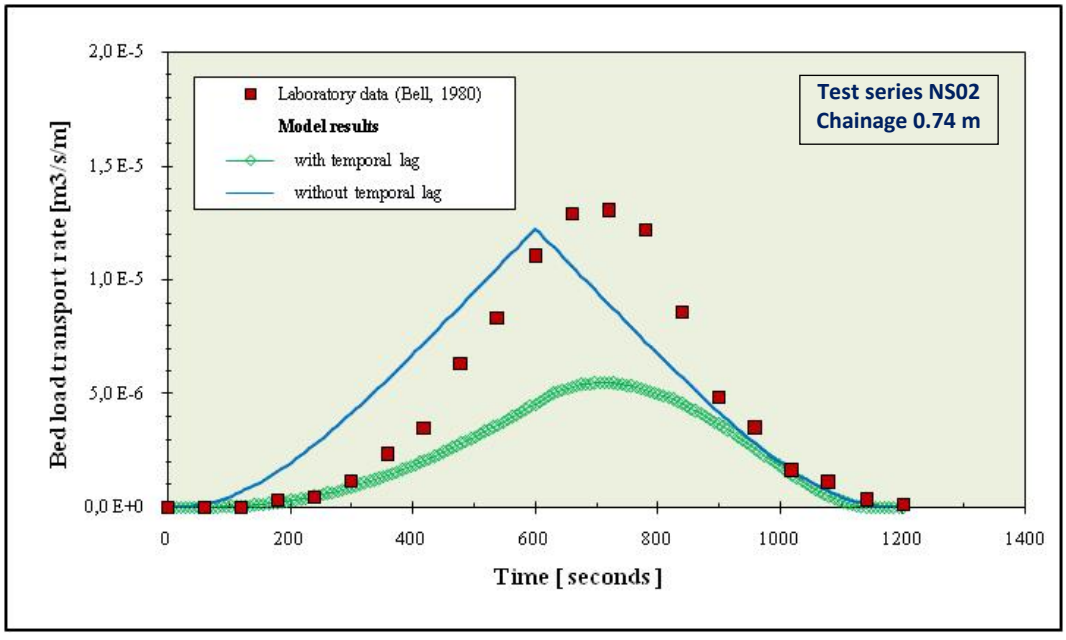

Figure 8.1 Effect of the inclusion of the temporal lag module on bed load transport for the NS02 series tests at chainage x = 0.74 m, using the coupled solution method with: Δt = 0.15 s, Cr_w = 0.41 - 0.60, Cr_s = 0.0 - 2.27 E-5 and Fr = 0.56 - 0.58.

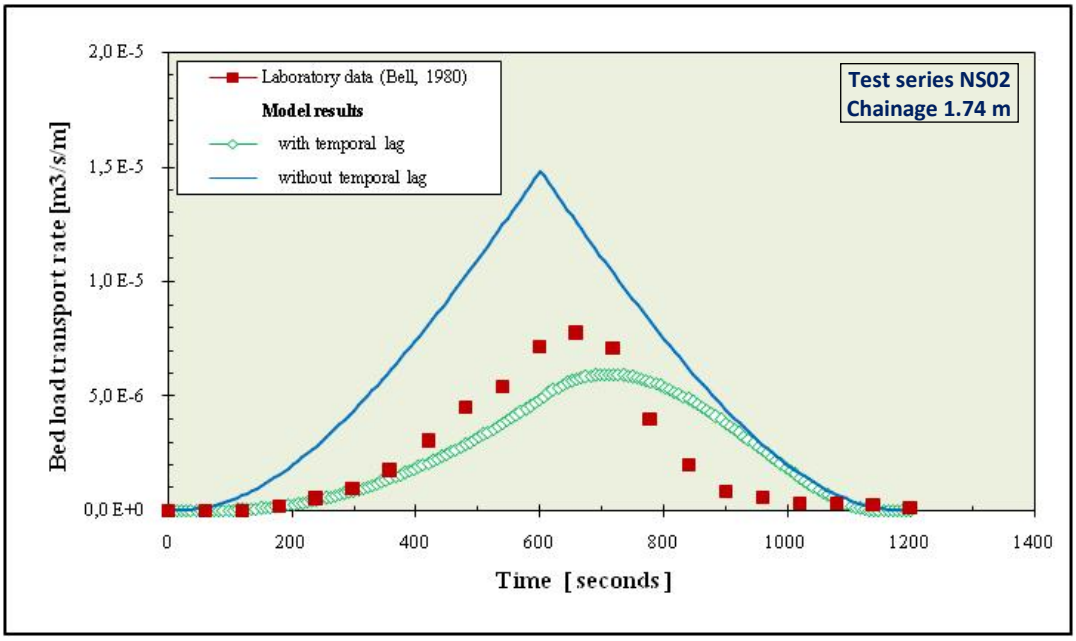

Figure 8.2 Effect of the inclusion of the temporal lag module on bed load transport for the NS02 series tests at chainage x = 1.74 m, using the coupled solution method with: Δt = 0.15 s, Cr_w = 0.41 - 0.60, Cr_s = 0.0 - 2.27 E-5 and Fr = 0.56 - 0.58.

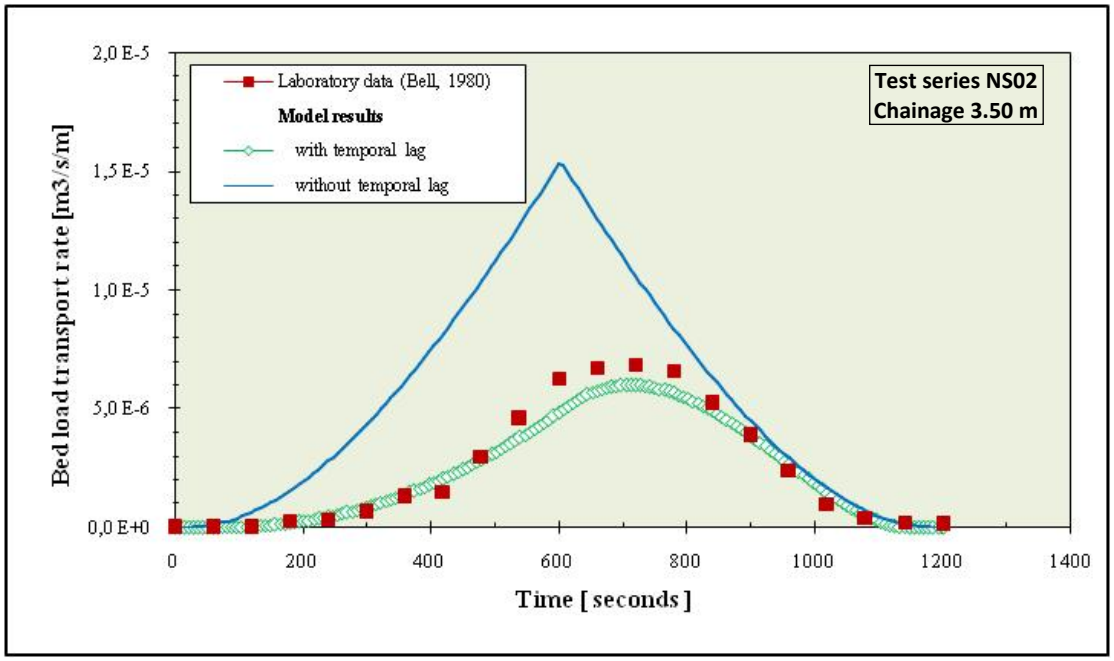

Figure 8.3 Effect of the inclusion of the temporal lag module on bed load transport for the NS02 series tests at chainage x = 3.50 m, using the coupled solution method with: Δt = 0.15 s, Cr_w = 0.41 - 0.60, Cr_s = 0.0 - 2.27 E-5 and Fr = 0.56 - 0.58.

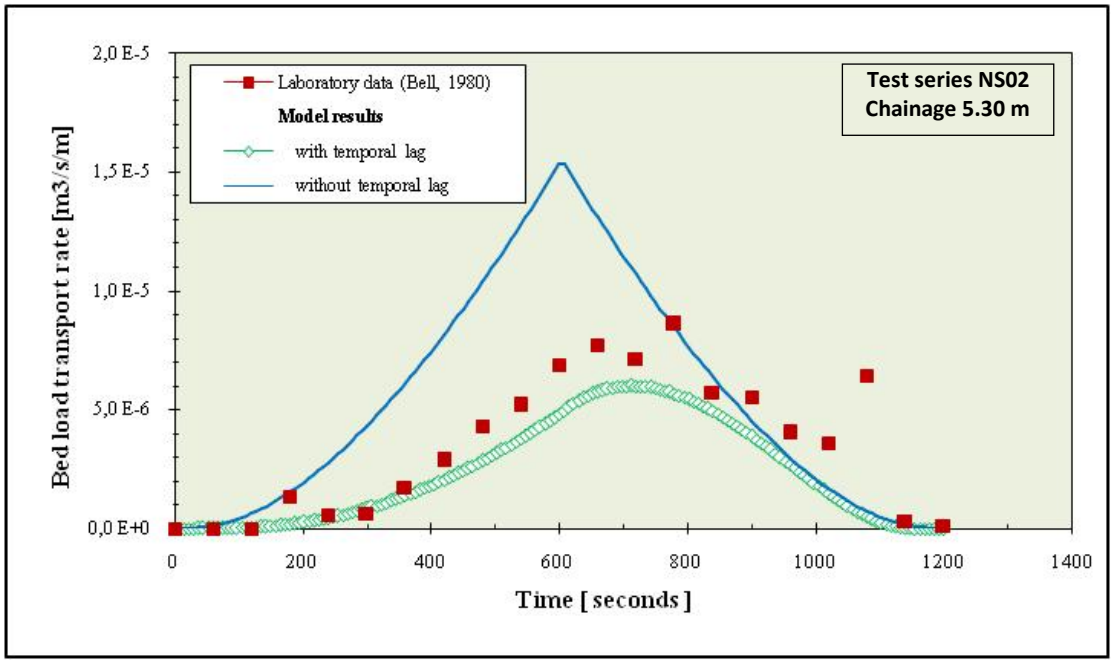

Figure 8.4 Effect of the inclusion of the temporal lag module on bed load transport for the NS02 series tests at chainage x = 5.30 *m*, using the coupled solution method with: Δt = 0.15 *s*, Cr_w = 0.41 - 0.60, Cr_s = 0.0 - 2.27 *E*-5 and Fr = 0.56 - 0.58.

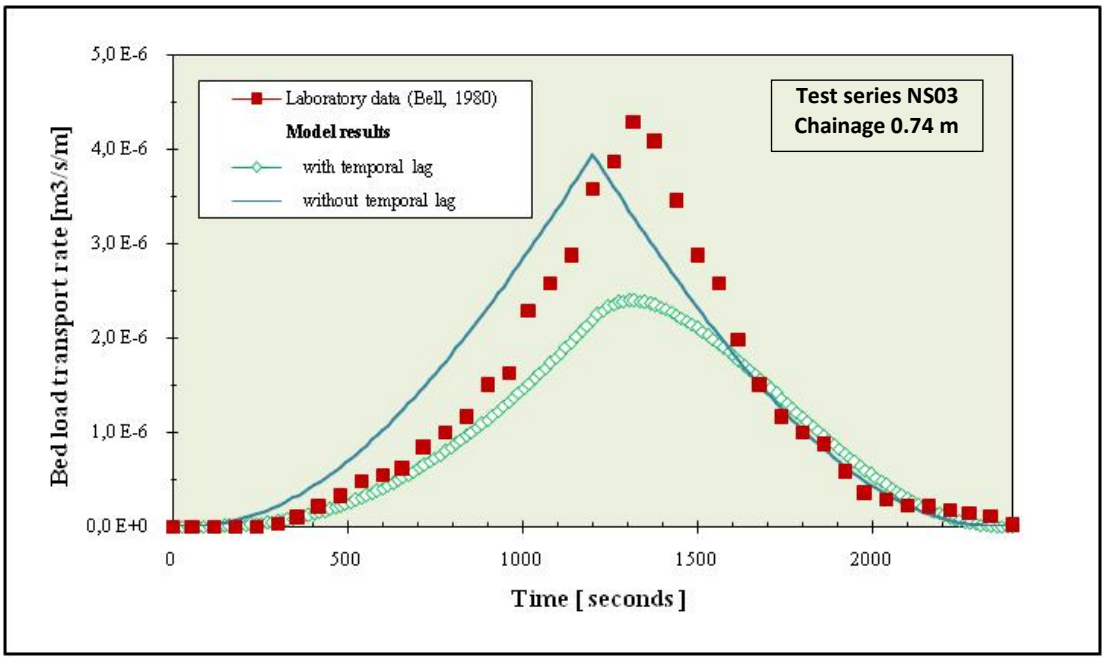

Figure 9.1 Effect of the inclusion of the temporal lag module on bed load transport for the NS03 series tests at chainage x = 0.74 *m*, using the coupled solution method with: Δt = 0.15 *s*, Cr_w = 0.41 - 0.56, Cr_s = 0.0 - 1.30 *E*-5 and Fr = 0.56 - 0.58.

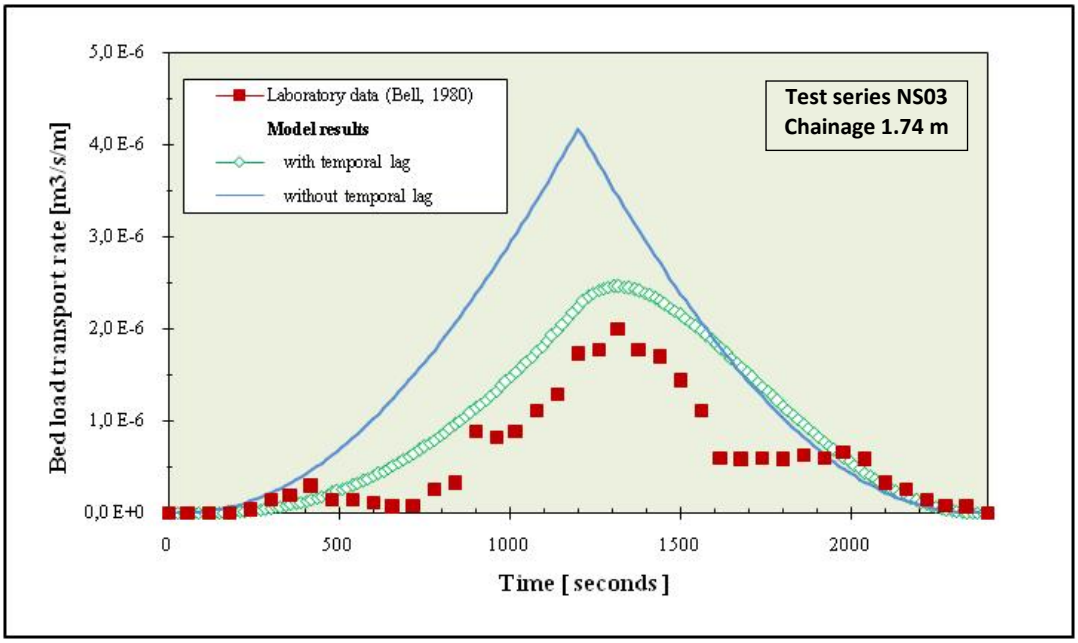

Figure 9.2 Effect of the inclusion of the temporal lag module on bed load transport for the NS03 series tests at chainage x = 1.74 *m*, using the coupled solution method with: Δt = 0.15 *s*, Cr_w = 0.41 - 0.56, Cr_s = 0.0 - 1.30 *E*-5 and Fr = 0.56 - 0.58.

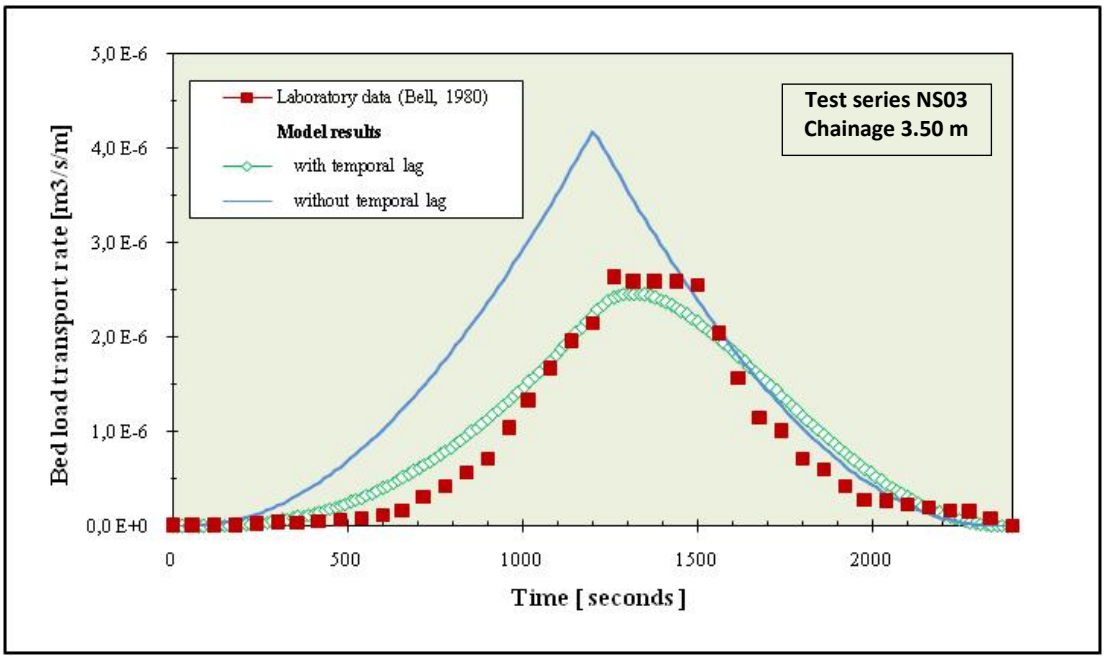

Figure 9.3 Effect of the inclusion of the temporal lag module on bed load transport for the NS03 series tests at chainage x = 3.50 *m*, using the coupled solution method with: Δt = 0.15 *s*, Cr_w = 0.41 - 0.56, Cr_s = 0.0 - 1.30 *E*-5 and Fr = 0.56 - 0.58.

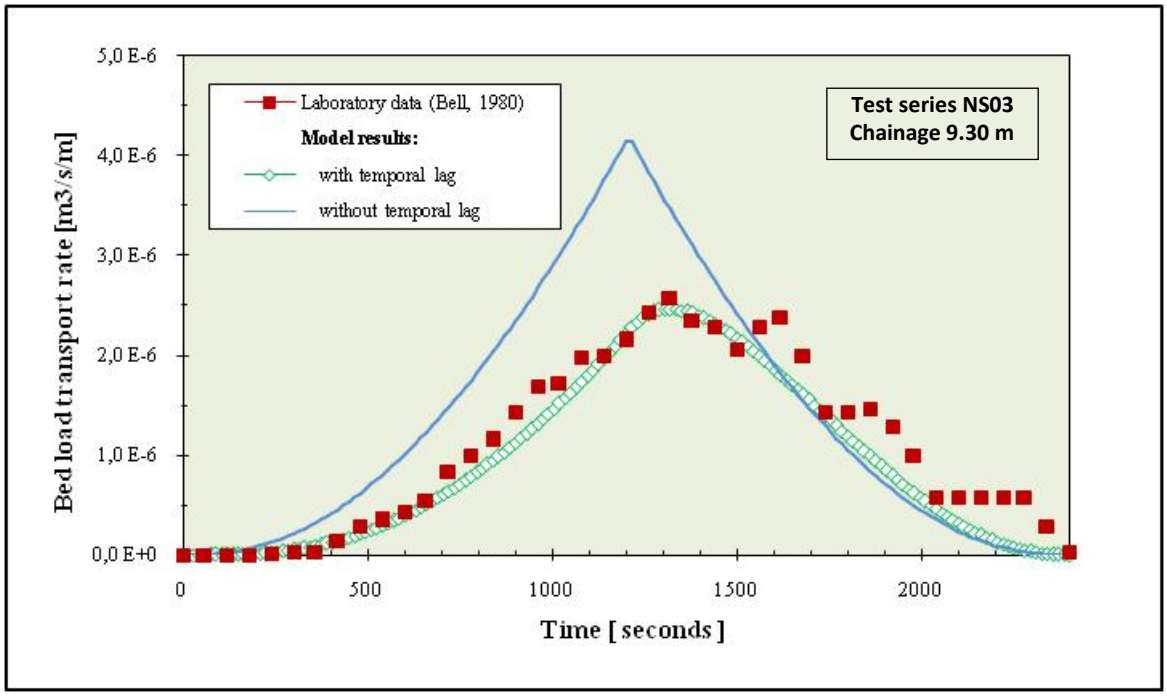

Figure 9.4 Effect of the inclusion of the temporal lag module on bed load transport for the NS03 series tests at chainage x = 9.30 m, using the coupled solution method with: Δt = 0.15 s, Cr_w = 0.41 - 0.56, Cr_s = 0.0 - 1.30 E-5 and Fr = 0.56 - 0.58.

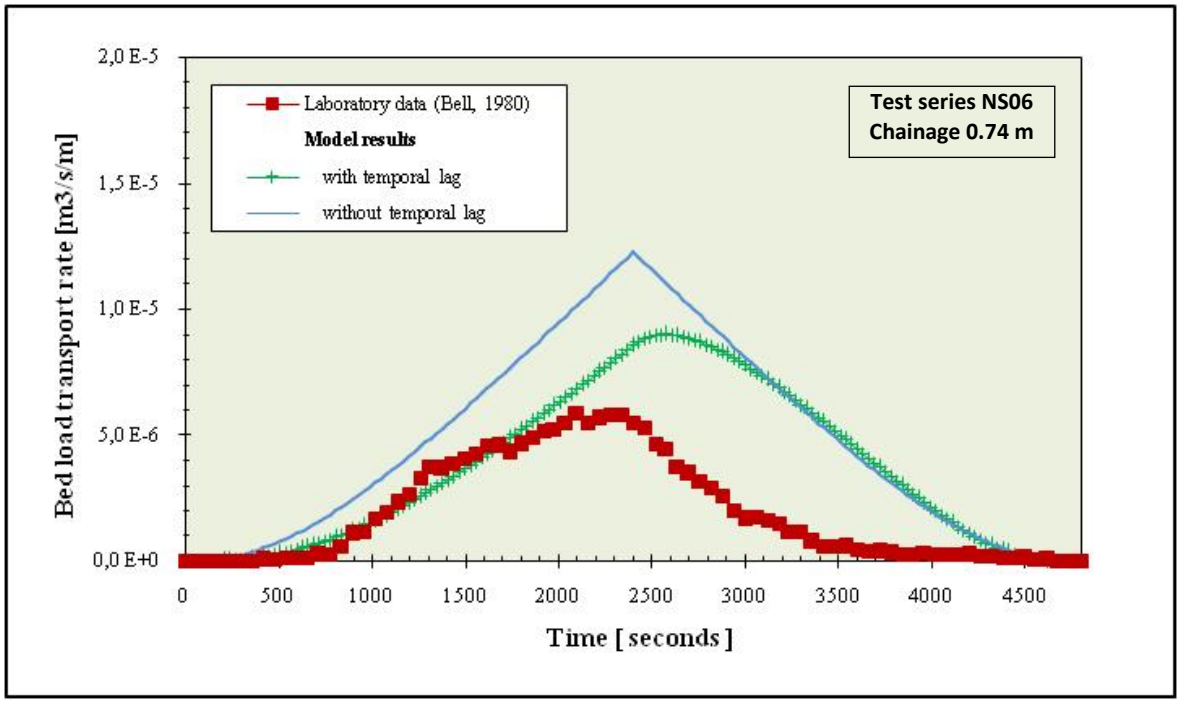

Figure 10.1 Effect of the inclusion of the temporal lag module on bed load transport for the NS06 series tests at chainage x = 0.74 m, using the coupled solution method with: Δt = 0.15 s, Cr_w = 0.41 - 0.60, Cr_s = 0.0 - 2.27 E-5 and Fr = 0.56 - 0.58.

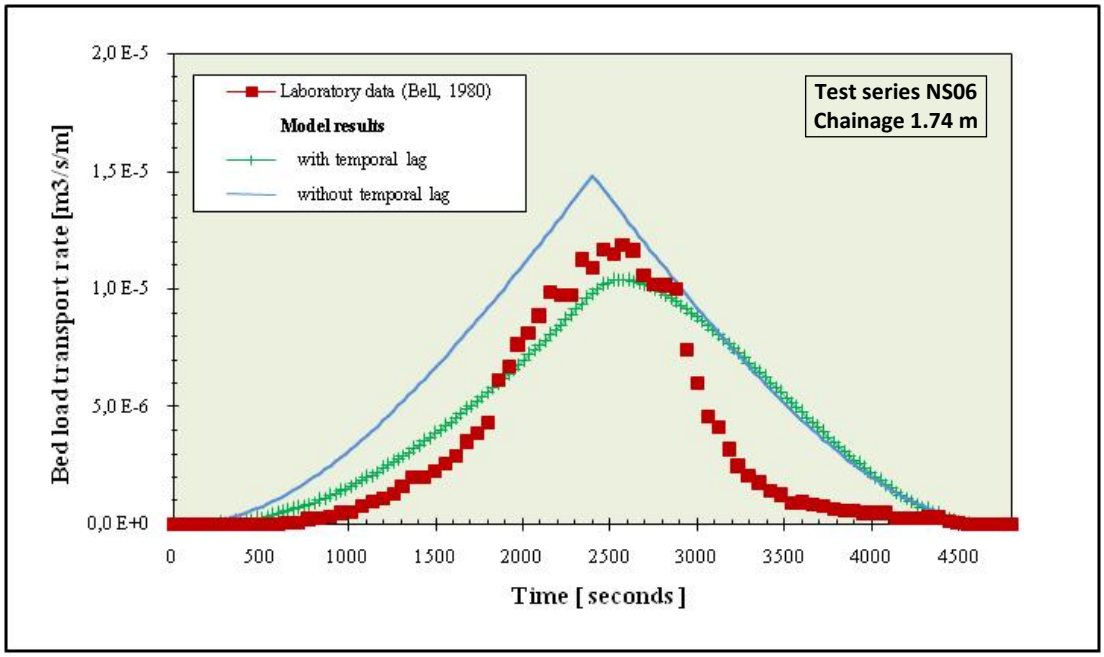

Figure 10.2 Effect of the inclusion of the temporal lag module on bed load transport for the NS06 series tests at chainage x = 1.74 *m*, using the coupled solution method with: Δt = 0.15 *s*, Cr_w = 0.41 - 0.60, Cr_s = 0.0 - 2.27 *E*-5 and Fr = 0.56 - 0.58.

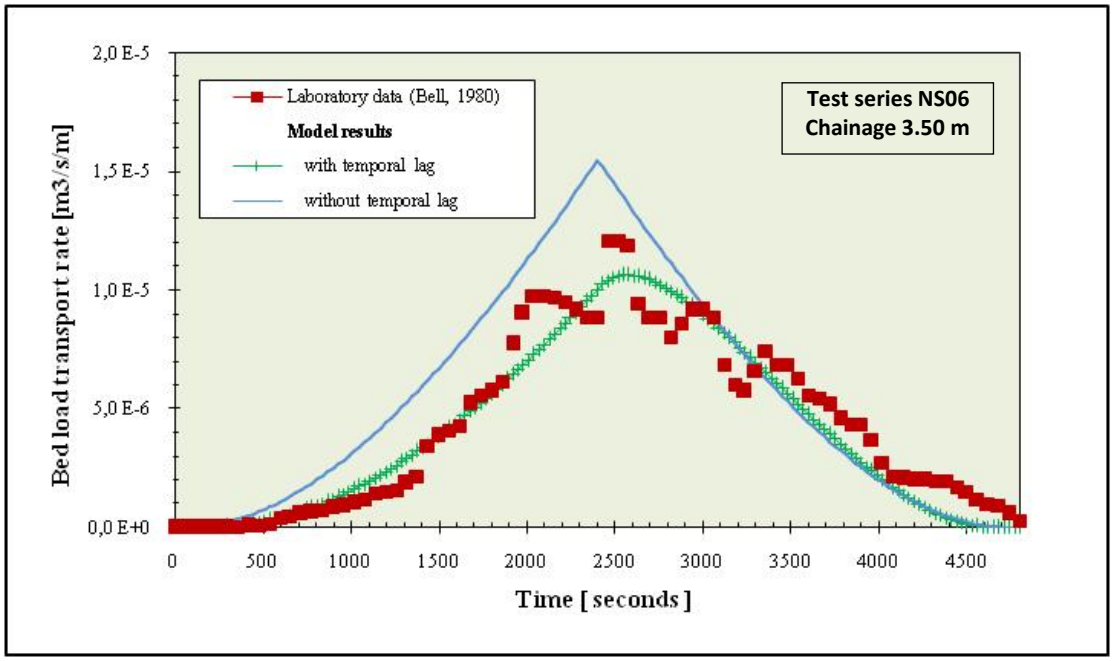

Figure 10.3 Effect of the inclusion of the temporal lag module on bed load transport for the NS06 series tests at chainage x = 3.50 *m*, using the coupled solution method with: Δt = 0.15 *s*, Cr_w = 0.41 - 0.60, Cr_s = 0.0 - 2.27 *E*-5 and Fr = 0.56 - 0.58.

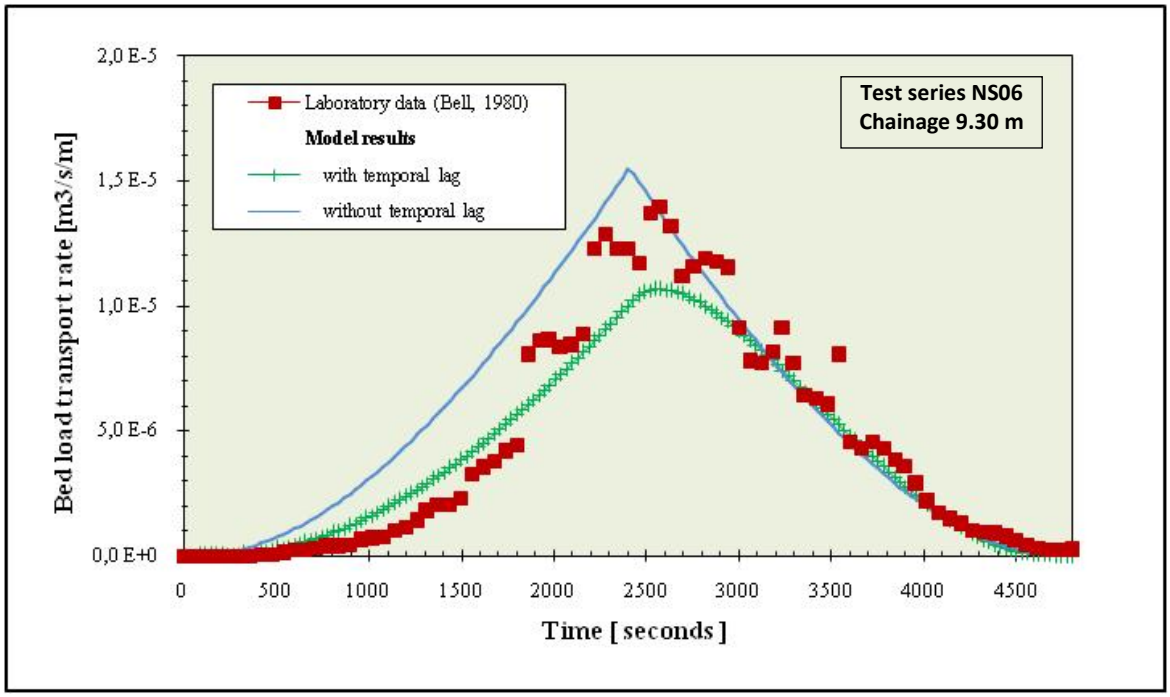

Figure 10.4 Effect of the inclusion of the temporal lag module on bed load transport for the NS06 series tests at chainage x = 9.30 m, using the coupled solution method with: Δt = 0.15 s, Cr_w = 0.41 - 0.60, Cr_s = 0.0 - 2.27 E-5 and Fr = 0.56 - 0.58.

CONCLUSIONS

The present study has resulted in the Bed Load Sub-model that has capabilities to analyze bed load sediment transport capacity under unsteady flow conditions by including the temporal lag as well as spatial lag effects of the alluvial reach.

The inclusion of spatial and temporal lags in the model significantly improves the predictive capability of the present model. These features are particularly needed to cope with non-equilibrium sediment transport conditions and the unsteadiness in the hydrodynamics. The spatial lag feature improves the model capability to resemble the non-linearity in the bed load sediment transport. The temporal lag sub-process enhances the model capability to simulate short term morphological change which, for an example, accompanies flashy flows.

The performance and robustness of the sub-model have been evaluated in simulating schematised field phenomena under unsteady conditions where temporal and spatial lag of alluvial system are present. Its prediction has been verified by laboratory data and shows its good agreement.

The effect of incorporating the temporal lag effect module is evident. For test with its steep hydrograph at the upstream boundary, the temporal lag module reduces the peak of the predicted bed load transport rate to almost a half compared with the module prediction which only incorporates the spatial lag effect module and give the prediction best match with the measured data.

RECOMMENDATIONS

The difficulty in measuring the bed load transport rate at sections where the bed level changes rapidly, should be solved by conducting several additional tests and follow up by statistical analysis. These additional tests are required to reconfirm the performance of the developed model.

This present study is only dealing with uniform bed materials. Since the selective transport, armored layer development and geometry of bed forms for rivers with non-uniform bed materials are integrally linked to the bed material transport and commonly found in rivers in Indonesia, hence the accuracy of simulating those phenomena will also influence the accuracy of analysis of flow depth, the bed load transport rate, the suspended load concentration and later on river morphology changes. This continuation study is proposed to be carried out.

REFERENCES

Bell, Robert G. 1980. Non-equilibrium bedload transport by steady and non-steady flows. University of Canterbury, Christchurch, New Zealand, PhD Thesis.

Bell, R.G. and A.J. Sutherland. 1983. Non equilibrium of bed load transport by steady flow. Journal of Hydraulic Research, IAHR, Vol 109, No. 3, pp. 351-367.

Goodwin, Peter. 1986. Sediment transport in unsteady flows. Report No. UBC/HEL-86/03, Hydraulic Engineering Laboratory, University of California, Berkeley, California, PhD Thesis.

Moerwanto, A.S. 2010. The Spatial Lag Effects of Bed Load Transport under Unsteady Flow Conditions, Jurnal Teknik Hidraulik, Vol. 1 No. 2, Desember 2010, pp. 95-107.

Phillips, B.C. 1984. Spatial and temporal lag effects in bed load sediment transport - Civil Engineering Research Report No. 84-10 - Reprint of PhD Thesis, Department of Civil Engineering, University of Canterbury.

Phillips, B. C. and A. J. Sutherland. 1989. Spatial lag effects in bed load sediment transport. Journal of Hydraulic Research, IAHR, Vol. 27, No. 1, pp. 115-133.

Phillips, B. C. and A. J. Sutherland. 1990. Temporal lag effects in bed load sediment transport. Journal of Hydraulic Research, IAHR, Vol. 28, No. 1, pp. 5-23.

Rijn, L.C. van. 1993. Principles of sediment transport in rivers, estuaries and coastal seas. Aqua Publications, Amsterdam.

Yalin, M.S. 1977. On the physical modelling of dunes. Proceedings of XVIIth Congress, IAHR, Baden-Baden, Vol. 1, Paper A4, pp. 25-32.